Negative Thermal Expansion in ZrW_2O_8: Mechanisms, Rigid Unit Modes, and Neutron Total Scattering

Matthew G. Tucker,[1,2] Andrew L. Goodwin,[1] Martin T. Dove,[1] David A. Keen,[3,2] Stephen A. Wells,[4] and John S. O. Evans[5]

[1]*Department of Earth Sciences, University of Cambridge, Downing Street, Cambridge CB2 3EQ, United Kingdom*
[2]*ISIS Facility, Rutherford Appleton Laboratory, Chilton, Didcot, Oxon OX11 0QX, United Kingdom*
[3]*Physics Department, Oxford University, Clarendon Laboratory, Parks Road, Oxford OX1 3PU, United Kingdom*
[4]*Biological Physics, Bateman Physical Sciences Building, Arizona State University, Tempe, Arizona 85287-1504, USA*
[5]*Department of Chemistry, University Science Laboratories, South Road, Durham DH1 3LE, United Kingdom*

(Received 24 August 2005; published 12 December 2005)

The local structure of the low-temperature ordered phase of the negative thermal expansion (NTE) material ZrW_2O_8 has been investigated by reverse Monte Carlo (RMC) modeling of neutron total scattering data. We obtain, for the first time, quantitative measurements of the extent to which the WO_4 and ZrO_6 polyhedra move as rigid units, and we show that these values are consistent with the predictions of rigid unit mode theory. We suggest that rigid unit modes are associated with the NTE. Our results do not support a recent interpretation of x-ray-absorption fine structure spectroscopy data in terms of a larger rigid structural component involving the Zr-O-W linkage.

DOI: 10.1103/PhysRevLett.95.255501 PACS numbers: 61.43.−j, 61.10.−i, 61.12.−q, 64.70.−p

Since 1996 ZrW_2O_8 has become established as one of the more important materials showing negative thermal expansion (NTE). In particular, ZrW_2O_8 has one of the highest negative coefficients of thermal expansion, -9.1×10^{-6} K^{-1} [$10 < T(K) < 300$], of NTE materials, the NTE is isotropic (because the crystal structure is cubic), and the NTE exists over a wide temperature range, 2–1035 K [1–3]. Accordingly, ZrW_2O_8 has been the subject of many recent studies, e.g., by neutron diffraction, spectroscopy, x-ray-absorption fine structure spectroscopy (XAFS), and computational modeling or theory. The crystal structure of ZrW_2O_8, Fig. 1, consists of a three-dimensional network of corner-linked ZrO_6 octahedra and WO_4 tetrahedra, with the latter having one nonbridging W-O bond. At high temperatures there is an onset of disorder with respect to the orientations of neighboring pairs of WO_4 tetrahedra, with an order-disorder phase transition at 448 K.

Much of the work on this material has focused on identifying the mechanism for the NTE. Several ideas now exist in the literature, and some of these have been reviewed [4]. Most models recognize that the existence of strong bonds play a role in the mechanism. The original idea was that along the Zr-O-W linkage, transverse vibrations of the O atoms, coupled with the fact that the Zr-O and W-O bond lengths have only a weak temperature dependence, will pull the Zr and W atoms closer together. Pryde *et al.* [5] argued that this model must be extended to take account of correlated motions within the structural polyhedra: rotations of the Zr-O and W-O bonds must be accompanied by whole-body rotations and translations of the ZrO_6 and WO_4 polyhedra. Whether a network structure can accommodate such correlated motions depends on the balance between the total number of degrees of freedom and the constraints imposed by the network connectivity. Pryde *et al.* demonstrated that the structure of ZrW_2O_8 has the flexibility to allow the existence of correlated polyhedral rotations [5]; when cast in the language of normal modes, such correlated motions are called "rigid unit modes" (RUMs).

More recently Cao *et al.* [6,7] have performed an analysis of XAFS data and proposed that the essentially rigid components of the structure are larger and composed of ZrO_6 and WO_4 units joined by rigid Zr-O-W linkages. This finding is based on the anomalously narrow Zr...W peaks in the Fourier transform of the XAFS spectra and their weaker than expected dependence on temperature. In fact, Cao *et al.* argue that these linkages are as stiff as the bonds within the ZrO_6 octahedra. It is not clear from their work *why* these linkages should be particularly rigid. In fact, our analysis suggests that if the Zr-O-W linkage is rigid, it will have the effect of stiffening the structure and inhibiting the motions responsible for NTE. From neutron total scattering experiments, the results of which will be discussed below, we find that the Zr...W linkages derived from peak widths in the pair distribution function do not appear to be as stiff as suggested by the XAFS results. Other experimental work has focused on the low-energy excitations, particularly through vibrational spectroscopic studies. Recent

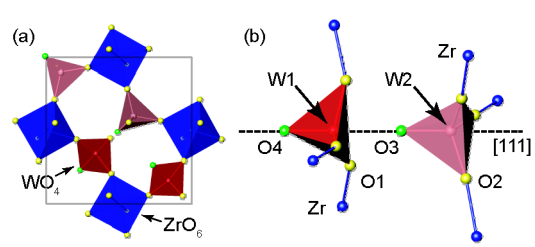

FIG. 1 (color online). Schematic diagram of the structure of the low-temperature α phase of ZrW_2O_8. (a) The arrangement of ZrO_6 octahedra and WO_4 tetrahedra. (b) Further detail of the environment around the unconnected WO_4 pairs and definition of a labeling scheme consistent with [3].

work [8] concludes that there is a significant translational component of the low-frequency vibrations; we comment on this point below.

In this Letter we are concerned with obtaining quantitative determinations of the type of phonon motions that give rise to NTE in ZrW_2O_8. Our main technique is neutron total scattering analyzed using the reverse Monte Carlo (RMC) method coupled with our recently developed analysis tools based on the formalism of geometric analysis (GA). The RMC-GA approach has proved to be highly useful in our analysis of other network-framework structures, two examples being the phase transitions in quartz [9] and $SrTiO_3$ [10]. The RMC-GA method enables us to extract a quantitative measurement of the fraction of the atomic dynamics that is accounted for by RUM motions and by motions that cause distortions of the structural polyhedra. This approach complements our formalism for analyzing the RUM spectra of network structures, based on our "split-atom" method [11].

Our neutron total scattering measurements were performed on the GEM [12] diffractometer at ISIS. This instrument is ideal for measurements over a wide range of scattering vector Q, with the large maximum value of Q of 50 $Å^{-1}$ giving an excellent resolution in real space ($\Delta r \simeq 0.1$ Å). In addition, the banks of high-angle detectors enable a high-resolution measurement of the Bragg diffraction pattern. In our use of the RMC method we combine the total scattering data—both the total scattering signal, $Qi(Q)$, and the pair distribution function, $D(r)$—with the Bragg diffraction data, treating both components as independent data sets. The total scattering data provide information about pair correlations (short-range order), the Bragg diffraction data provide information about single-atom distribution functions (long-range order), and its hkl dependence introduces a three-dimensional component. Our approach is described in some detail in other publications [13], and the specific details of this experiment and analysis will also be published elsewhere. In this Letter we focus on the analysis of data collected for temperatures below 300 K in order to avoid complications associated with the order-disorder phase transition described above. The RMC method generates atomic configurations that are consistent with these experimental data, and therefore the configurations replicate the likely short-range and long-range order in the material. An example of the fit to the $D(r)$ data is shown in Fig. 2. These configurations can then be analyzed to give information about particle correlations. When considering rotations it has to be admitted that these involve correlations of higher order than probed in these experiments (and, in fact, in any experiment that can be performed), but we have strong evidence to suggest that in these types of structures the knowledge of the single particle and pair distributions are effective constraints on the possible configurations that can be generated by the RMC method. The GA method enables us to extract the rotational, translational, and distortive motions of the structural polyhedra from the RMC configurations directly.

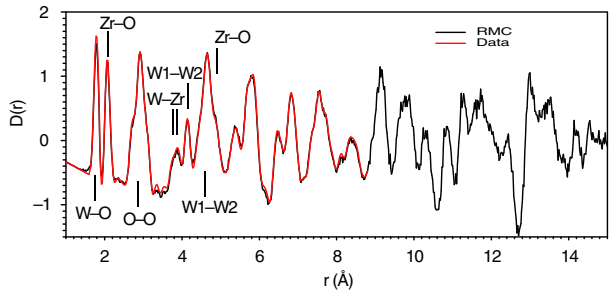

FIG. 2 (color online). Pair distribution function, $D(r)$, of ZrW_2O_8, obtained by direct Fourier transform of the total scattering data and from the RMC simulations. Principal contributions to the low-r features are labeled.

In addition to the RMC analysis, we also perform Rietveld analysis of the Bragg diffraction data. This directly gives the average positions of the atoms (in fact, we can extract the same information from the RMC configurations). The important point here is that we can obtain information about fluctuations of interatomic distances. Suppose we have two atoms labeled A and B. The pair distribution function (or direct analysis of the RMC configuration) gives the mean instantaneous distance between these atoms, which we label as $\langle A\text{-}B\rangle$. In contrast, analysis of the structures obtained by Rietveld refinement gives the distance between mean positions of the atoms, which we label as $\langle A\rangle\text{-}\langle B\rangle$. In our previous work on phases of silica, the large difference between $\langle A\text{-}B\rangle$ and $\langle A\rangle\text{-}\langle B\rangle$ is a clear signature of the large fluctuations of the orientations of the SiO_4 tetrahedra. We compare results for $\langle A\text{-}B\rangle$ and $\langle A\rangle\text{-}\langle B\rangle$ for several important A and B pairs at a temperature of 10 K in Table I. The polyhedral W-O and Zr-O σ^2, and the higher-distance W…W σ^2 scale well as a function of atomic separation. The W1…O3 peak σ^2 is roughly twice as large for its separation in comparison, and the Zr…W peak σ^2 values are lower in comparison. The W1…O3 separation has greater flexibility because these atoms are separated by a larger number of linkages around the network, whereas there is only one linkage involved in the Zr…W separation. In general, our values for σ^2 are larger than those from the XAFS data [6,7]. Both total scattering and XAFS peak widths, to some extent, will be affected by issues in the Fourier transform, particularly related to the maximum value of the scattering vector. However, we believe that the XAFS σ^2 values are consistently too small. This can be seen by comparing σ^2 from the XAFS data in Table I with 4 times the variance of distances that are averaged during the XAFS analysis [14]. For example, for the range of W-O bonds, the crystallographic data would suggest a value for the XAFS σ^2 of 0.005 $Å^2$; the XAFS value is 5 times lower. Similarly, the XAFS σ^2 values for the Zr-O and Zr…W peaks are too low by factors of 4 and 10, respectively. The Zr…W values are important in the discussion developed by Cao *et al.* [6,7] and commented on below. Although absolute values of the σ^2 values may be affected by the Fourier transformation

TABLE I. Summary of bond lengths and additional atom pair distances (in Å) of ZrW_2O_8 at 10 K determined from Rietveld refinement and RMC modeling. *A-B* and *A* . . . *B* refer to bonded atoms and atom pair distances, respectively. The W1. . .W2 distances are separated into the distance between W1 and W2 within the unlinked pairs and the shortest W1. . .W2 distance around the network via one ZrO_6 octahedron. The two Zr. . .Zr pair distances were not separated in the analysis of the RMC models. In addition, the peak width parameter, σ^2 (in $Å^2$), is also shown for pair distributions from RMC models and XAFS data [6,7]; in several cases (e.g., W-O) the results from XAFS average over crystallographically distinct pairs. For a definition of the atom labels see Fig. 1.

	Rietveld $\langle A\rangle$-$\langle B\rangle$	RMC $\langle A\rangle$-$\langle B\rangle$	RMC $\langle A\text{-}B\rangle$	RMC $\sigma^2_{\langle A\text{-}B\rangle}$	XAFS $\sigma^2_{\langle A\text{-}B\rangle}$
W1-O1	1.8136(7)	1.8093	1.813	0.0042	0.001
W1-O4	1.7217(15)	1.6898	1.716	0.0035	
W1. . .O3	2.3910(19)	2.4320	2.404	0.0092	
W2-O2	1.7848(7)	1.7874	1.789	0.0031	
W2-O3	1.7211(18)	1.7438	1.751	0.0038	
Zr-O1	2.0410(10)	2.0731	2.068	0.0034	0.002
Zr-O2	2.1086(10)	2.0935	2.088	0.0039	
W1. . .Zr	3.7586(6)	3.7631	3.760	0.0053	0.003
W2. . .Zr	3.8845(7)	3.8730	3.870	0.0046	
W1 . . . $W2_{pair}$	4.1123(17)	4.1773	4.155	0.0102	0.004
W1 . . . $W2_{network}$	4.6485(8)	4.6203	4.625	0.0098	0.008
Zr. . .Zr	6.4757(11)	6.4594	6.491	0.0060	0.005
Zr. . .Zr	6.5060(11)				

process, the variation of σ^2 with temperature should be more robust. It is expected that $\sigma^2 \propto k_B T \omega^{-2}$ in the classical limit, where ω^2 is inversely proportional to the (effective) stiffness of a particular separation. In Fig. 3 we plot the σ^2 values of some of the important contact distances, as per Table I, as functions of temperature. Our results are different from the XAFS results in one important regard. The XAFS data have the variation of σ^2 with temperature for Zr. . .W linkages nearly identical to the variation of σ^2 for the Zr-O peaks ($\sim 7 \times 10^{-6}$ $Å^2\,K^{-1}$). Our total scattering data show a much larger variation in temperature for the σ^2 of the Zr. . .W linkages (22, 9, 3.7, and 1.6 for W1. . .Zr, W2. . .Zr, Zr-O1, and Zr-O2, respectively, all $\times 10^{-6}$ $Å^2\,K^{-1}$).

The conclusion we draw from the σ^2 values and their variation with temperature is that the Zr. . .W linkages are not particularly stiff, in contrast with the conclusions of Cao *et al.* [6,7]. Based on our data, we suggest that this linkage has lower flexibility than other linkages merely because it is a short linkage within the network. Nevertheless, it is able to flex in response to the overall flexibility of the network, and it does not play a significant role in stiffening the network.

We now turn to the GA analysis of the flexibility of the network of linked ZrO_6 and WO_4 polyhedra (see Fig. 4). This analysis provides measurements of the proportion of the atomic motions due to rigid-body rotations and translations, and it also gives a comparison between the rigid-body motions and the motions that cause deformations of the structural polyhedra. It is instructive to compare the data of Fig. 4 with a similar analysis on quartz [9], although noting that the present data are for relatively low temperatures. In quartz, the rigid-body motions of the SiO_4 tetrahedra were associated with RUM excitations, and on

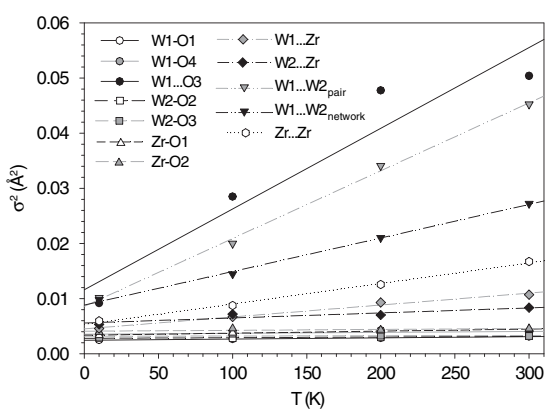

FIG. 3. Temperature dependence of the widths of various peaks in the pair distribution functions obtained from the RMC analysis.

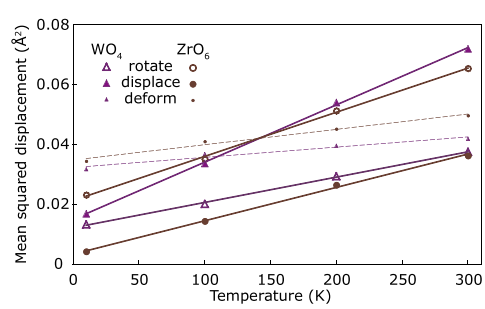

FIG. 4 (color online). Temperature dependence of the mean-square amplitudes of the rotational, translational, and distortive motions of the ZrO_6 octahedra and WO_4 tetrahedra obtained using our GA algorithms.

TABLE II. Calculated components of the RUM motions from GA analysis of RMC configurations and using a split-atom model [11].

	RMC-GA				Split-atom
	10 K	100 K	200 K	300 K	···
WO_4 Rotation	0.30	0.26	0.24	0.23	0.36
ZrO_6 Rotation	0.26	0.22	0.21	0.20	0.12
WO_4 Translation	0.38	0.43	0.44	0.45	0.39
ZrO_6 Translation	0.06	0.09	0.11	0.12	0.13

heating from low temperature there is a rapid increase in the RUM contributions. In ZrW_2O_8 there is also a significant contribution from the rigid-body motions, and these increase rapidly on heating. (The results for the modes that involve deformations of the polyhedra are probably overestimates because these motions absorb most of the data errors in the RMC analysis; this is indicated by the low variation with temperature.) The large increase in the RUM amplitudes on heating points to the fact that they are associated with low frequencies. Also, the translational components of the RUM motions are as significant as the rotational components [15]. This is consistent with the conclusion of [8]. Furthermore, Fig. 4 shows that the WO_4 tetrahedra are slightly stiffer than the ZrO_6 octahedra. From a split-atom analysis [11] we have calculated the fraction of the RUM motions that are associated with rotations and translations of the two types of polyhedra, obtaining the values in Table II. The key point from this table is that in spite of the gross simplification in the split-atom model, the relative components of the translation and rotation rigid unit motions predicted by the split-atom model are in reasonable agreement with the results of the GA analysis. This consistency between theory and data analysis lends support to the idea that RUM motions are important in ZrW_2O_8. We note that we have also adapted the split-atom calculation to include a stiff Zr. . .W linkage; this stiffness completely removes the RUM flexibility of the network. As noted above, the basic RUM model for NTE is based on the idea that rotations of linked polyhedra will pull them in towards each other; this motion will be seen more locally as the flexing of the Zr-O-W linkage through transverse motions of the O atom, without significant stretching of the Zr-O and W-O bonds in the manner originally suggested by Mary *et al.* [2]. What the RUM model of NTE achieves is to provide a mechanism whereby the whole network has the flexibility to allow these transverse motions to occur without an energy penalty associated with accompanying distortions of the polyhedra [16]. The results of this Letter, which presents the first study of the structural behavior of ZrW_2O_8 over both short- and long-range length scales simultaneously, demonstrate the important role of RUMs in the dynamics of this material, and show that other more-complex speculations are unwarranted.

We acknowledge financial support from EPSRC and Trinity College Cambridge (A. L. G.).

[1] J. S. O. Evans, T. A. Mary, T. Vogt, M. A. Subramanian, and A. W. Sleight, Chem. Mater. **8**, 2809 (1996).
[2] T. A. Mary, J. S. O. Evans, T. Vogt, and A. W. Sleight, Science **272**, 90 (1996).
[3] J. S. O. Evans, W. I. F. David, and A. W. Sleight, Acta Crystallogr. Sect. B **55**, 333 (1999).
[4] G. D. Barrera, J. A. O. Bruno, T. H. K. Barron, and N. L. Allan, J. Phys. Condens. Matter **17**, R217 (2005).
[5] A. K. A. Pryde, K. D. Hammonds, M. T. Dove, V. Heine, J. D. Gale, and M. C. Warren, J. Phys. Condens. Matter **8**, 10 973 (1996).
[6] D. Cao, F. Bridges, G. R. Kowach, and A. P. Ramirez, Phys. Rev. Lett. **89**, 215902 (2002).
[7] D. Cao, F. Bridges, G. R. Kowach, and A. P. Ramirez, Phys. Rev. B **68**, 014303 (2003).
[8] J. N. Hancock, C. Turpen, Z. Schlesinger, G. R. Kowach, and A. P. Ramirez, Phys. Rev. Lett. **93**, 225501 (2004).
[9] S. A. Wells, M. T. Dove, M. G. Tucker, and K. Trachenko, J. Phys. Condens. Matter **14**, 4645 (2002)—most of the atomic motions in β quartz are due to RUMs, causing considerable amplitudes for the rotations of the SiO_4 tetrahedra and dynamic disorder, consistent with the results of our theoretical RUM analysis.
[10] Q. Hui, M. G. Tucker, M. T. Dove, S. A. Wells, and D. A. Keen, J. Phys. Condens. Matter **17**, S111 (2005)—the RUM component of the atomic motions is much smaller than in quartz, consistent with our theoretical analysis.
[11] A. P. Giddy, M. T. Dove, G. S. Pawley, and V. Heine, Acta Crystallogr. Sect. A **49**, 697 (1993)—the core of the method is a dynamical matrix whose components are determined by how much the motions of linked polyhedra will stretch the shared atom. RUMs are observed as the zero-frequency eigensolutions. The dynamical matrix yields a density of states in which the effective frequency-squared measures the extent to which phonon modes involve distortions of the polyhedra.
[12] A. C. Hannon, Nucl. Instrum. Methods Phys. Res., Sect. A **551**, 88 (2005).
[13] M. G. Tucker, M. T. Dove, and D. A. Keen, J. Appl. Crystallogr. **34**, 630 (2001); M. T. Dove, M. G. Tucker, and D. A. Keen, Eur. J. Mineral. **14**, 331 (2002).
[14] A factor of 4 arises because the XAFS and total scattering σ values are the widths of the distributions of pair separations, whereas the standard deviation of bond lengths corresponds to half the equivalent width.
[15] This statement does not impact on the idea that the rotational components of the RUMs are responsible for the NTE. The translations allow the structure to accommodate the rotations.
[16] There are easily understood exceptions to this. For example, the related ZrV_2O_7-type materials have no RUMs [5], but here there is an energy driving deformation of the V-O-V linkages that offsets the energy penalty associated with the necessary distortions of the ZrO_6 octahedra. We have demonstrated this structurally in the related material ZrP_2O_7 using the same methodology as here, to be reported elsewhere.